AIP | Applied Physics Letters

Investigation of geometric design in piezoelectric microelectromechanical systems diaphragms for ultrasonic energy harvesting

Qiongfeng Shi, Tao Wang, Takeshi Kobayashi, and Chengkuo Lee

Citation: Applied Physics Letters **108**, 193902 (2016); doi: 10.1063/1.4948973
View online: http://dx.doi.org/10.1063/1.4948973
View Table of Contents: http://scitation.aip.org/content/aip/journal/apl/108/19?ver=pdfcov
Published by the AIP Publishing

APPLIED PHYSICS LETTERS **108**, 193902 (2016)

Investigation of geometric design in piezoelectric microelectromechanical systems diaphragms for ultrasonic energy harvesting

Qiongfeng Shi,[1,2] Tao Wang,[1,2] Takeshi Kobayashi,[3] and Chengkuo Lee[1,2,a)]
[1]*Department of Electrical and Computer Engineering, National University of Singapore, 4 Engineering Drive 3, Singapore 117583*
[2]*Center for Sensors and MEMS, National University of Singapore, 4 Engineering Drive 3, Singapore 117583*
[3]*National Institute of Advanced Industrial Science and Technology (AIST), 1-2-1 Namiki, Tsukuba, Ibaraki 305-8564, Japan*

(Received 5 March 2016; accepted 28 April 2016; published online 9 May 2016)

Acoustic energy transfer (AET) has been widely used for contactless energy delivery to implantable devices. However, most of the energy harvesters (ultrasonic receivers) for AET are macro-scale transducers with large volume and limited operation bandwidth. Here, we propose and investigate two microelectromechanical systems diaphragm based piezoelectric ultrasonic energy harvesters (PUEHs) as an alternative for AET. The proposed PUEHs consist of micro-scale diaphragm array with different geometric parameter design. Diaphragms in PUEH-1 have large length to width ratio to achieve broadband property, while its energy harvesting performance is compromised. Diaphragms in PUEH-2 have smaller length to width ratio and thinner thickness to achieve both broadband property and good energy harvesting performance. Both PUEHs have miniaturized size and wide operation bandwidth that are ideally suitable to be integrated as power source for implantable biomedical devices. PUEH-1 has a merged -6 dB bandwidth of 74.5% with a central frequency of 350 kHz. PUEH-2 has two separate -6 dB bandwidth of 73.7%/30.8% with central frequencies of 285 kHz/650 kHz. They can adapt to various ultrasonic sources with different working frequency spectrum. Maximum output power is 34.3 nW and 84.3 nW for PUEH-1 and PUEH-2 at 1 mW/cm^2 ultrasound intensity input, respectively. The associated power density is 0.734 μW/cm^2 and 4.1 μW/cm^2, respectively. Better energy harvesting performance is achieved for PUEH-2 because of the optimized length to width ratio and thickness design. Both PUEHs offer more alignment flexibility with more than 40% power when they are in the range of the ultrasound transmitter. *Published by AIP Publishing.*
[http://dx.doi.org/10.1063/1.4948973]

Aiming at realizing sustainable self-powered wireless sensor networks or implantable systems, various piezoelectric energy harvesters from macro-scale to micro-scale are developed.[1–9] Shen *et al*. reported a unimorph piezoelectric energy harvester with resonant frequency of 461.15 Hz.[1] Liu *et al.* developed a microelectromechanical systems (MEMS) based energy harvester for low-frequency vibrations from 30 to 47 Hz.[2] Lee *et al.* presented two cantilever-type piezoelectric microelectromechanical systems (MEMS) generators working on d_{31} mode and d_{33} mode with resonant frequencies of 255.9 Hz and 214 Hz, respectively.[3] Dagdeviren *et al.* proposed a implantable energy harvester to scavenge heart, lung, and diaphragm vibrations (1 to 2 Hz).[4] Most reported devices harvest vibration energy from human motions or machine vibrations in low frequency range. To harvest high frequency vibration energy of propagating acoustic/ultrasonic wave, acoustic energy transfer (AET) has been developed.[10,11] In AET, ultrasonic energy is transferred from ultrasonic transmitter to ultrasonic receiver. Compared to other wireless power transfer technologies, i.e., inductive power transfer (IPT), AET is more advantageous. IPT is not able to deliver energy through conductive medium and has limited working distance.[12] More importantly, electromagnetic wave is associated with safety issues for human body, which is not allowed to contain high power. AET, on the other hand, is able to transfer energy through a conductive medium over a large distance.[13] Moreover, ultrasonic wave has minimum side effects on tissues, which makes AET ideally suitable for powering implantable biomedical devices.[14,15]

However, most existing ultrasonic receivers (energy harvesters) in AET are macro-scale bulk lead zirconate titanate (PZT) transducers.[16–19] Miniaturized size of energy harvesters is always preferable to facilitate system-level integration. The large size of conventional ultrasonic receiver weakens its integration capability. Although micro-scale piezoelectric ultrasonic transducers have been reported, they have not been adopted for energy harvesting yet.[20,21] In addition, different existing ultrasound sources have different working frequencies. For example, 20–400 kHz is for ultrasound cleaning, 0.5–10 MHz is for ultrasonic flaw detection, and 1–18 MHz is for diagnostic sonography, etc. However, conventional ultrasonic receiver has limited operation bandwidth due to the large acoustic impedance mismatch with soft tissue. When the ultrasonic frequency is not match with the resonant frequency of conventional ultrasonic receiver, its power decreases dramatically. Therefore, micro-scale broadband ultrasonic energy harvesters are more desirable and can be applied to different situations which require various kinds of working frequencies.

In general, when ultrasonic energy harvesters used in highly damped medium like water or soft tissue, the amplitude

[a)]Author to whom correspondence should be addressed. Electronic mail: elelc@nus.edu.sg

versus frequency response spectrum shows broadband characteristics if frequency bandwidth merges of different resonant modes. A piezoelectric MEMS diaphragm based ultrasonic transducer achieves optimized broadband property (-6 dB bandwidth of 95%) by combining a few adjacent resonant peaks into one broad peak.[20] Although broadband property of the piezoelectric MEMS diaphragm based ultrasonic transducer is achieved, its energy harvesting performance still has not been studied. Therefore, piezoelectric MEMS rectangular diaphragm based ultrasonic energy harvesters are worth for further investigation in terms of geometric related parameters. Most previously reported piezoelectric diaphragm based energy harvesters are not MEMS based diaphragms, and all are circular diaphragms that can only work at fundamental resonant frequency.[22–26] Rectangular diaphragm allows more design freedom than the circular diaphragm in terms of geometry design. The first geometric parameter is length to width ratio of diaphragm. Large length to width ratio facilitates the excitation of several resonant modes in a narrower frequency range to achieve mode-merging broadband property. The second geometric parameter is thickness of diaphragm. Thinner thickness can further reduce the acoustic impedance mismatch with medium. Thus bandwidth of each resonant mode is broadened. But variation of length to width ratio or thickness also has influence on the energy harvesting performance. Therefore, in this letter, two MEMS diaphragm based piezoelectric ultrasonic energy harvesters (PUEHs) with different geometric parameter design are first proposed. Then, both broadband property and energy harvesting performance of the proposed PUEHs are profoundly investigated.

Device structure of the proposed PUEH is illustrated in Figure 1(a). Both PUEHs consist of 7 diaphragms that are connected in parallel. Dimensions of the diaphragms in PUEH-1 and PUEH-2 are $250\,\mu m \times 1550\,\mu m$ and $250\,\mu m \times 500\,\mu m$, respectively. Each diaphragm is a multilayer structure with Si ($10\,\mu m$ for PUEH-1 and $5\,\mu m$ for PUEH-2), $1\,\mu m$ SiO_2, 200 nm Pt, $2\,\mu m$ PZT, and 200 nm Pt, as in Figure 1(b). Photograph of the fabricated PUEH-1 and PUEH-2 on a finger is shown in Figure 1(c). Effective size of the PUEH-1 and PUEH-2 is 4.67 mm^2 and 2.06 mm^2, respectively, as indicated by the red dash rectangle. Both PUEHs are much smaller than conventional bulk PZT receivers with diameters in centimeters range.[15–18] Scanning electron microscope (SEM) images of the PUEH-1 are shown in Figures 1(d) and 1(e), and SEM images of PUEH-2 are shown in Figures 1(f) and 1(g), respectively.

Fabrication of the PUEHs starts from a silicon-on-insulator (SOI) wafer with Si ($10\,\mu m$ for PUEH-1 and $5\,\mu m$ for PUEH-2)/SiO_2 ($1\,\mu m$)/Si ($400\,\mu m$). A $1\,\mu m$ oxide is first sputtered on top. Then, Pt (200 nm)/Ti (10 nm) layers are deposited as bottom electrode by DC magnetron sputtering. After that, a $2\,\mu m$ PZT layer is formed by sol-gel process. Another Pt (200 nm)/Ti (10 nm) layers are then deposited as the top electrode. Next, top electrode, PZT, and bottom electrode are etched subsequently. Electrodes are etched by Ar ions and PZT is etched by a mixture of HF, HNO_3, and HCl. Lastly, backside Si and SiO_2 layers are etched by deep reactive-ion etching (DRIE) to release the diaphragm.

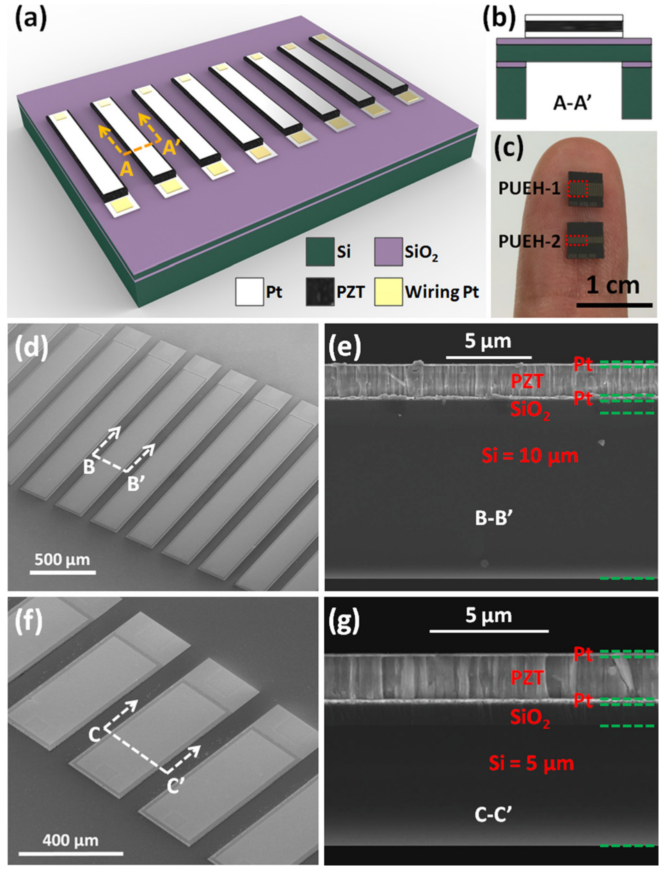

FIG. 1. Device structure of the proposed MEMS based PUEHs: (a) 3-D schematic illustration of the PUEH; (b) Cross-sectional view of the multilayer diaphragm structure; (c) Photograph of PUEH-1 and PUEH-2 on a human finger; (d) Bird view SEM image and (e) cross-sectional view SEM image of PUEH-1; (f) Bird view SEM image and (g) cross-sectional view SEM image of PUEH-2.

Based on the model proposed by Wang *et al.*,[20] for fully clamped rectangular diaphragm (dimension: $L_x = L$ and $L_y = k \times L$, k is length to width ratio of the diaphragm), modal frequencies of resonant modes are given by

$$f_{m,1} = f_0 \times \sqrt{\left(\frac{m^2 + k^2}{k^2 + 1}\right)}, \tag{1}$$

where f_0 is the fundamental frequency and m is the positive integer that denotes the resonant mode of the diaphragm ($m = 1, 2, 3\ldots$). The interval of adjacent frequencies is decided by k. The interval becomes smaller when k is larger, which means frequencies of high order resonant modes are getting closer to the fundamental frequency. Thus the number of resonant modes in a certain frequency range can be controlled by k to facilitate mode-merging broadband property.

Design of diaphragm array ($250\,\mu m \times 1550\,\mu m$) in PUEH-1 is based on this theory that large length to width ratio can achieve broadband property. Bandwidth can also be broadened by thinner thickness design because thinner thickness enables less acoustic impedance mismatch with medium. Thus diaphragm array ($250\,\mu m \times 500\,\mu m$) with thinner thickness in PUEH-2 is designed to achieve similar broadband property and good energy harvesting performance. Broadband property and energy harvesting performance of these two designs are then investigated.

The fabricated $250\,\mu m \times 1550\,\mu m$ and $250\,\mu m \times 500\,\mu m$ diaphragms are first characterized in air by a holographic

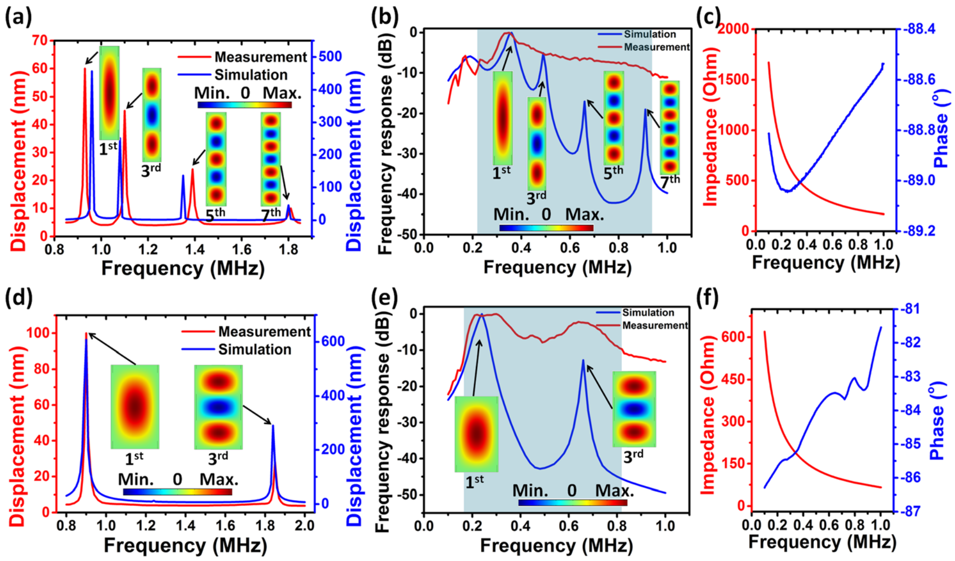

FIG. 2. Device characterization of PUEH-1 and PUEH-2: Frequency response of the fabricated diaphragm in PUEH-1 measured (a) in air and (b) in water; (c) Impedance of the fabricated diaphragm in PUEH-1 measured in water. Frequency response of the fabricated diaphragm in PUEH-2 measured (d) in air and (e) in water; (f) Impedance of the fabricated diaphragm in PUEH-2 measured in water.

MEMS analyzer (DHMR2100, Lyncee Tec Ltd.). The PZT composite diaphragms are excited by 1 Vpp electrical signal. Measured frequency responses in air of the two devices are shown in Figures 2(a) and 2(d), respectively. Finite elements model (FEM) is built by COMSOL Multiphysics software to simulate frequency response of the diaphragms. Simulation results under 1 Vpp sinusoidal electrical excitation are also shown and compared in Figures 2(a) and 2(d). Frequency deviation of simulation and measurement is due to small fabrication error of the diaphragm structure. Inset of Figures 2(a) and 2(d) shows different mode shapes of diaphragm vibration. Four resonant modes (1st, 3rd, 5th, and 7th mode) of $250\,\mu m \times 1550\,\mu m$ diaphragm can be excited from 0.9 MHz to 1.85 MHz. Two resonant modes (1st and 3rd mode) of $250\,\mu m \times 500\,\mu m$ diaphragm can be excited from 0.85 MHz to 1.9 MHz. More resonant modes can be excited in the similar frequency bandwidth with larger length to width ratio based on Eq. (1). It can be observed that larger maximum displacement is achieved for $250\,\mu m \times 500\,\mu m$ diaphragm. This is mainly because of two reasons. First, larger length to width ratio has more constrain on diaphragm vibration and thus smaller maximum displacement. Second, diaphragm with thinner thickness is softer and more sensitive under the same excitation. It is worth to note that the even resonant modes are missing in the frequency response spectrum. This is because in the even resonant modes, the diaphragm can be divided into symmetrical regions with opposite motions. But, the mechanical force from converse piezoelectric effect is unidirectional which cannot be coupled to such opposite motion to excite the even resonant modes.

Then, PUEH-1 and PUEH-2 are immersed in a water tank filled with de-ionized (DI) water. Sinusoidal signal (10 Vpp) is applied for ultrasound generation, and a hydrophone (2118, Precision Acoustic Ltd.) is used to measure the ultrasound pressure. Frequency responses of $250\,\mu m \times 1550\,\mu m$ and $250\,\mu m \times 500\,\mu m$ diaphragms from measurement and simulation are shown in Figures 2(b) and 2(e), respectively. The four excited resonant modes of $250\,\mu m \times 1550\,\mu m$ diaphragm are getting closer to the fundamental frequency when operated in largely damped water medium. They merge together and form a wide operation bandwidth from 220 kHz to 930 kHz (light blue background in Figure 2(b)). PUEH-1 has a -6 dB bandwidth of 74.5% with a central resonant frequency of 350 kHz. Meanwhile, two broadened resonant modes of $250\,\mu m \times 500\,\mu m$ diaphragm are excited in similar frequency range. Each resonant mode is broadened because thinner thickness enables less acoustic impedance mismatch with water medium. The two broadened resonant modes merge with each other, leading to a comparable wide operation bandwidth from 170 kHz to 820 kHz (light blue background in Figure 2(e)). PUEH-2 has two large -6 dB bandwidth of 73.7%/30.8% with central frequencies of 285 kHz/650 kHz for 1st/3rd resonant mode. Difference of simulation and measurement results in Figures 2(b) and 2(e) is mainly due to the limitation of the software and small dimension deviation by fabrication. The highly damped water lowers the Q factor of each mode. The peak of each mode thus becomes not sharp and they are overlapped together. However, the software cannot take all the damping effects into account, and hence the peaks in simulation have higher Q factors which look sharper. Both PUEH-1 and PUEH-2 with different geometric parameter design are able to achieve excellent broadband property.

Impedances of $250\,\mu m \times 1550\,\mu m$ and $250\,\mu m \times 500\,\mu m$ diaphragms measured in water are shown in Figures 2(c) and 2(f), respectively. Seven diaphragms in PUEH-1 and PUEH-2 are connected in parallel, respectively, in order to match the internal impedance with a common $50\,\Omega$ resistor load. To demonstrate the energy harvesting capability of the proposed PUEHs, an AET system is built as illustrated in Figure 3(a). A commercialized bulk PZT transducer (M165D25, Prowave corp.) is functioned as a transmitter, and the designed PUEH-1 and PUEH-2 is receiver. They are immersed in DI water with 1 cm separation distance. The bulk PZT transmitter is connected to a waveform generator. Sinusoidal signal with amplitude of 10 Vpp and frequency varying from 100 kHz to 1 MHz is applied to the transmitter for ultrasound generation. The receiver is connected to a $50\,\Omega$ resistor load and an oscilloscope for voltage measurement.

Since ultrasound pressure from the bulk PZT transmitter varies with respect to frequency, the output voltage and

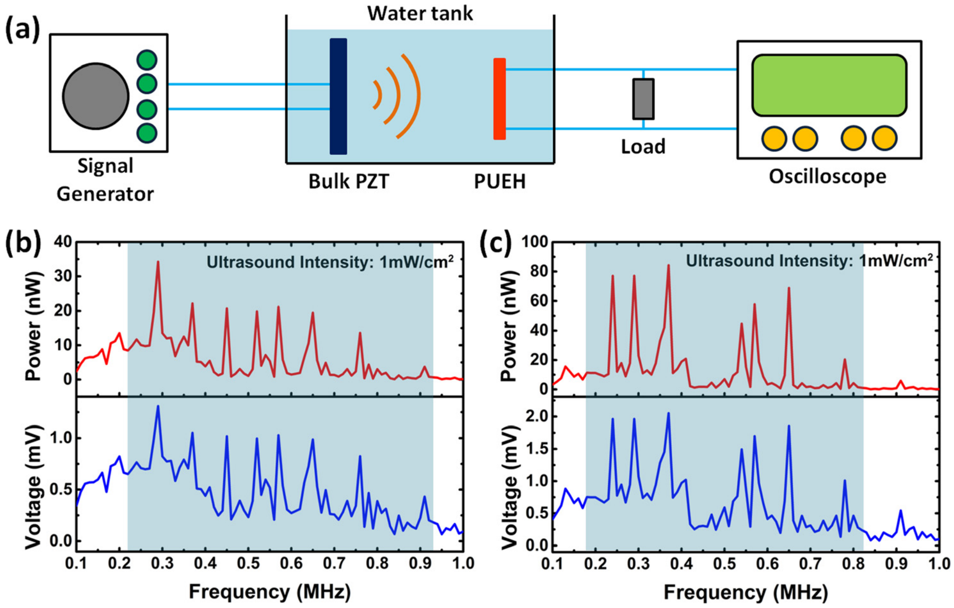

FIG. 3. Energy harvesting test: (a) Testing setup for voltage and power measurement of PUEH-1 and PUEH-2; Output voltage and power of (b) PUEH-1 and (c) PUEH-2 on a 50 Ω resistor load.

power are normalized to 1 mW/cm^2 ultrasound intensity in order to provide a fair comparison. The ultrasound intensity can be calculated from ultrasound pressure measured by hydrophone using equation[27]

$$I = \frac{P^2}{2Z}, \tag{2}$$

where I is the ultrasound intensity, P is the ultrasound pressure, and Z is the acoustic impedance of medium (Z is 1.48 $\times$ 10^6 kg/m^2·s for water). Figures 3(b) and 3(c) show the output voltage and power of PUEH-1 and PUEH-2 on the 50 Ω resistor load, respectively. Benefited from the broadband property, both PUEH-1 and PUEH-2 can harvest energy in a wide frequency range. PUEH-1 can operate from 220 kHz to 930 kHz (light blue background in Figure 3(b)), and PUEH-2 can operate from 170 kHz to 820 kHz (light blue background in Figure 3(c)). The maximum normalized output power for PUEH-1 and PUEH-2 is 34.3 nW at 290 kHz and 84.3 nW at 370 kHz, respectively. The associated power density for PUEH-1 and PUEH-2 is 0.73 μW/cm^2 (17.62 μW/cm^3) and 4.09 μW/cm^2 (99.90 μW/cm^3), respectively. Even though PUEH-2 has slightly smaller operation bandwidth compared to PUEH-1, its energy harvesting performance is much better. Smaller length to width ratio has less constrain on diaphragm vibration, and thus larger maximum displacement is achieved. Moreover, diaphragm with thinner thickness is more sensitive to the incoming ultrasonic wave, further enabling better energy harvesting performance. Hence, PUEH-2 is more optimized in terms of both broadband property and energy harvesting performance. Compared to reported MEMS energy harvesters with power density of 33 μW/cm^3,[2] 28.5 μW/cm^3,[7] and 159.4 μW/cm^3,[8] PUEH-2 shows comparable or better energy harvesting performance even when input ultrasound pressure is low (1 mW/cm^2 input ultrasound intensity). In practical energy transferring, higher ultrasound intensity can be applied to further improve the output power. According to the United States Food and Drug Administration (FDA), the safety limit of ultrasound intensity is 720 mW/cm^2. If ultrasound intensity of 700 mW/cm^2 is applied, PUEH-1 and PUEH-2 would produce power of 24.01 μW and 59.01 μW, respectively. It is worth noting that within the operation bandwidth of PUEH-1 and PUEH-2, the output voltage and power are not smooth curves as the frequency response curves. This could be because of the standing wave between transmitter and receiver in the AET system.

Alignment is an important issue for IPT. Even a small misalignment of two coils could drastically drop the power transferring efficiency. Therefore, the capability of the PUEHs to scavenge energy when it is not aligned with the ultrasound source is studied. Figure 4(a) shows the testing setup for alignment test where PUEH is moved along x-axis with respect to the ultrasound transmitter. PUEH-1 and PUEH-2 show similar behavior in the alignment test. Figure 4(b) shows the power of

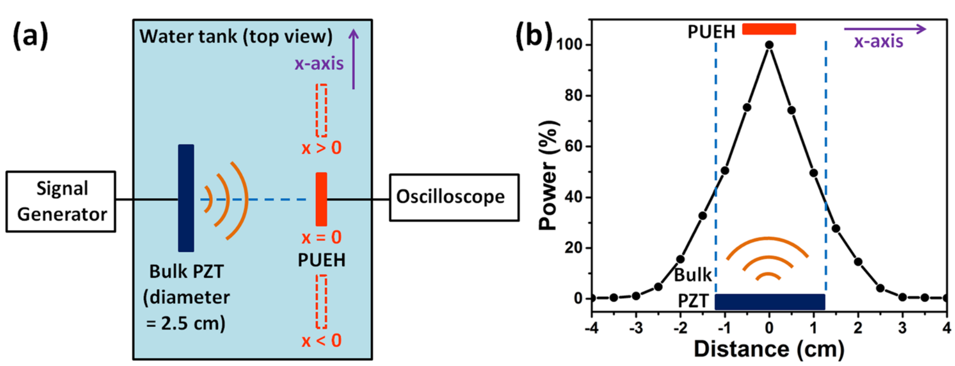

FIG. 4. Alignment test: (a) Testing setup for alignment test when PUEH is moved along x-axis with respect to the ultrasound transmitter; (b) Power of PUEH-2 when it is moved along x-axis.

PUEH-2 when it is moved along x-axis. The power of PUEH-2 decreases when it is moved sideways from ultrasound transmitter. As long as PUEH-2 is in the range of the ultrasound transmitter (diameter of 2.5 cm), the generated power is above 40% with respect to maximum power. When PUEH-2 is out of the ultrasound transmitter range, the power drops rapidly. Therefore, in practical application, as long as we can maintain the PUEH in the range of the ultrasound transmitter, more than 40% power can be achieved, which allows more alignment flexibility.

In conclusion, two MEMS diaphragm based broadband PUEHs with different geometric design are proposed and investigated. Benefited from length to width ratio and thickness design, both PUEHs have excellent broadband property. PUEH-1 has a large −6 dB bandwidth of 74.5% with a central frequency of 350 kHz. PUEH-2 has two large −6 dB bandwidth of 73.7%/30.8% with central frequencies of 285 kHz/650 kHz for 1st/3rd resonant mode. PUEH-1 can harvest energy from 220 kHz to 930 kHz, and PUEH-2 can harvest energy from 170 kHz to 820 kHz. Maximum output power at 1 mW/cm^2 ultrasound intensity input is 34.3 nW and 84.3 nW for PUEH-1 and PUEH-2, respectively. The associated power density is 0.734 μW/cm^2 and 4.1 μW/cm^2, respectively. PUEH-2 shows much better energy harvesting performance and comparable wide operation bandwidth due to the optimized length to width ratio and thickness design. Both PUEHs offer more alignment flexibility in practical application with more than 40% power as long as they are in the range of the ultrasound transmitter. Therefore, both PUEH-1 and PUEH-2 show great potential as efficient broadband ultrasonic energy harvesters to replace the conventional bulk receivers in AET for various implantable biomedical devices.

This work is supported by NRF2011 NRF-CRP001-057 Program "Self-powered body sensor for disease management and prevention-orientated healthcare" (R-263-000-A27-281) from the National Research Foundation (NRF), Singapore.

[1]D. Shen, J.-H. Park, J. Ajitsaria, S.-Y. Choe, H.-C. Wikle, and D. J. Kim, J. Micromech. Microeng. **18**(5), 055017 (2008).
[2]H. Liu, C. J. Tay, C. Quan, T. Kobayashi, and C. Lee, J. Microelectromech. Syst. **20**(5), 1131 (2011).
[3]B. S. Lee, S. C. Lin, W. J. Wu, X. Y. Wang, P. Z. Chang, and C. K. Lee, J. Micromech. Microeng. **19**(6), 065014-1 (2009).
[4]C. Dagdeviren, B. D. Yang, Y. Su, P. L. Tran, P. Joe, E. Anderson, J. Xia, V. Doraiswamy, B. Dehdashti, X. Feng, B. Lu, R. Poston, Z. Khalpey, R. Ghaffari, Y. Huang, M. J. Slepian, and J. A. Rogers, Proc. Natl. Acad. Sci. U.S.A. **111**(5), 1927 (2014).
[5]J. C. Park, J. Y. Park, and Y. P. Lee, J. Microelectromech. Syst. **19**(5), 1215 (2010).
[6]R. Elfrink, T. M. Kamel, M. Goedbloed, S. Matova, D. Hohlfeld, Y. van Andel, and R. van Schaijk, J. Micromech. Microeng. **19**(9), 094005-1 (2009).
[7]H. Liu, S. Zhang, T. Kobayashi, T. Chen, and C. Lee, Micro Nano Lett. **9**(4), 286 (2014).
[8]H. Liu, C. Lee, T. Kobayashi, C. J. Tay, and C. Quan, Sens. Actuators, A **186**, 242 (2012).
[9]X. Wang, J. Song, J. Liu, and Z. L. Wang, Science **316**(5821), 102 (2007).
[10]M. G. L. Roes, J. L. Duarte, M. A. M. Hendrix, and E. A. Lomonova, IEEE Trans. Ind. Electron. **60**(1), 242 (2013).
[11]M. P. Kazmierkowski and A. J. Moradewicz, in *15th International Power Electronics and Motion Control Conference* (EPE/PEMC) (2012), p. Session 3-1.
[12]E. Waffenschmidt and T. Staring, in *13th European Conference on Power Electronics and Applications* (EPE) (2009), p. 1.
[13]Y. Hu, X. Zhang, J. Yang, and Q. Jiang, IEEE Trans. Ultrason., Ferroelectr., Freq. Control **50**(7), 773 (2003).
[14]P. J. Larson and B. C. Towe, in *5th International IEEE/EMBS Conference on Neural Engineering* (NER) (2011), p. 265.
[15]T. Maleki, N. Cao, S. H. Song, C. Kao, S.-C. A. Ko, and B. Ziaie, IEEE Trans. Biomed. Eng. **58**(11), 3104 (2011).
[16]S. Ozeri, D. Shmilovitz, S. Singer, and C.-C. Wang, Ultrasonics **50**(7), 666 (2010).
[17]S. Q. Lee, W. Youm, and G. Hwang, Proc. Meet. Acoust. **19**(1), 030030 (2013).
[18]S. Suzuki, S. Kimura, T. Katane, H. Saotome, O. Saito, and K. Kobayashi, Jpn. J. Appl. Phys., Part 1 **41**(5S), 3600 (2002).
[19]H. Kawanabe, T. Katane, H. Saotome, O. Saito, and K. Kobayashi, Jpn. J. Appl. Phys., Part 1 **40**(5S), 3865 (2001).
[20]T. Wang, T. Kobayashi, and C. Lee, Appl. Phys. Lett. **106**(1), 013501 (2015).
[21]T. Wang, R. Sawada, and C. Lee, IEEE Electron Device Lett. **36**(9), 957 (2015).
[22]C. Mo, L. J. Radziemski, and W. W. Clark, Smart Mater. Struct. **19**(7), 075010 (2010).
[23]X. Chen, T. Yang, W. Wang, and X. Yao, Ceram. Int. **38**, S271 (2012).
[24]F. Liu, A. Phipps, S. Horowitz, K. Ngo, L. Cattafesta, T. Nishida, and M. Sheplak, J. Acoust. Soc. Am. **123**(4), 1983 (2008).
[25]S. B. Horowitz, M. Sheplak, L. N. Cattafesta III, and T. Nishida, J. Micromech. Microeng. **16**(9), S174 (2006).
[26]I. Kuehne, D. Marinkovic, G. Eckstein, and H. Seidel, Sens. Actuators, A **142**(1), 292 (2008).
[27]P. R. Hoskins, K. Martin, and A. Thrush, *Diagnostic Ultrasound: Physics and Equipment* (Cambridge University Press, 2010).